THz STREAK CAMERA FOR FEL TEMPORAL DIAGNOSTICS: CONCEPTS AND CONSIDERATIONS

Pavle Juranić, Rafael Abela, Rasmus Ischebeck, Luc Patthey, Claude Pradervand, Milan Radović,
Volker Schlott, Andrey Stepanov, PSI, Villigen PSI, Switzerland
Ishkhan Gorgisyan, Christoph P. Hauri, Leonid Rivkin,
PSI, Villigen PSI, Switzerland, and EPFL, Lausanne, Switzerland
Balazs Monoszlai, PSI, Villigen PSI, Switzerland, and University of Pécs, Hungary
Rosen Ivanov, Peter Peier, DESY, Hamburg, Germany
Jia Liu, XFEL.EU, Hamburg, Germany
Kanade Ogawa, Shigeki Owada, Tadashi Togashi, Makina Yabashi,
RIKEN SPring-8 Center, Sayo-cho, Sayo-gun, Hyogo, Japan

Abstract

The accurate measurement of the arrival time of a hard x-ray free electron laser (FEL) pulse with respect to a laser is of utmost importance for pump-probe experiments proposed or carried out at FEL facilities around the world. This paper presents the latest device to meet this challenge, a THz streak camera, and discusses the challenges in its design, use, and analysis of results.

INTRODUCTION

Laser pump, x-ray probe experiments performed at FEL facilities around the world [1, 2, 3, 4, 5] typically want to use short pulse length and intense coherent x-ray radiation to perform experiments with sub-picosecond time resolution. As they go towards improved temporal resolutions, the experiments require accurate measurements of the arrival times of the FEL pulses relative to a laser pump on the sample they are probing. This measurement must also be non-invasive, allowing the experimenters the maximum use of the X-ray beam for their work rather than for diagnostics.

Several methods have been proposed and implemented in the past to meet this diagnostics challenge: transmission/reflectivity spatial and spectral encoding used for soft and hard x-rays at FLASH, SACLA, and LCLS [6, 7, 8, 9], the THz streak camera for soft x-rays at FLASH [10, 11] and other methods [12, 13, 14]. These methods all have their advantages and drawbacks, and the only one that has been attempted for hard x-ray arrival time measurement is the spatial/spectral encoding setup, which has an arrival time accuracy of on the order of 10 fs RMS [6, 9]. The potentially more accurate THz streak camera has not been attempted for use at hard x-ray sources due to the small photoionization cross-section of the gas target and the difficulties in differentiating jitters in the photon energy of the FEL beam from an arrival time signal of the FEL beam by electron spectroscopy. The Photon Arrival and Length Monitor (PALM) prototype chamber [15] developed at the Paul Scherrer Institute (PSI) for the future SwissFEL facility mitigates both of these problems, measuring the pulse length, and the arrival times of hard x-ray FEL pulses relative to a THz pulse and the laser it is generated from.

CONCEPTS

The concept of the THz streak camera has been explained in the past in literature [16, 17, 18], and has shown itself capable of measuring pulse lengths of high-harmonic-generation (HHG) soft x-rays in table-top laser laboratories. The device can also be used to measure the arrival time of the x-ray relative to the THz pulse.

The THz streak camera uses a gas that is photoionized by the x-ray light as an electron emitter. The electrons are then subject to a time-varying vector potential generated by co-propagating THz radiation, the duration of which is longer than the pulse length of the x-ray pulse. A shift in the arrival time of the x-ray pulse translates to a shift in the kinetic energy gained by the electrons in the vector potential. The final kinetic energy of the photoelectrons K_f streaked by the vector potential U_p is

$$K_f = K_0 + 2U_p sin^2(\varphi_0) \pm \sqrt{8K_0U_p}\sin(\varphi_0) \qquad (1)$$

where K_0 is the initial kinetic energy of the electrons at the time of ionization, φ_0 is the phase of the vector potential at the time of the ionization, and

$$U_p = \frac{e^2E_{THz}^2(t)}{4m_e\omega_{THz}^2} \qquad (2)$$

$E_{THz}(t)$ is the (sinusoidal) THz electric field, e is the electron charge, m_e is the mass of the electron, and ω_{THz} is the frequency of the THz f in radians/s.

The time delay between the external THz field and the FEL pulse was controlled by a translation stage, and time of flight of the electrons under different time delays were recorded, forming a two dimensional (2D) streaked spectrogram. As shown in Eq. 1, the shape of the spectrogram is determined by the THz frequency, initial electron kinetic energy and the vector potential. The time-to-energy map can be extracted by recording the center of mass (COM) kinetic energy of each time delay and shot-to-shot arrival time of the FEL pulses related to the THz pulse are retrieved by recording the single-shot electron kinetic energy when the stage is set at the middle of the time-to-energy slope. The pulse lengths are measured by looking at the change in spectral width of

ISBN 978-3-95450-133-5

the kinetic energy of the electrons. A longer pulse will give a longer width, as described in [10, 11].

Since x-ray photoionization cross sections decrease as the x-ray photon energy increases [19], fewer electrons are thus expected to generate from single-shot ionization of the noble gas atoms for hard x-rays. However, the PALM setup counterbalanced this effect by using gas from a supersonic pulsed valve [20] that is synchronized to the FEL pulse that increases the sample density in the interaction region, while in the other hand decrease the gas load in the streaking chamber.

SETUP CONSIDERATIONS

The flight path of electrons, and especially low-kinetic-energy electrons, can be affected by magnetic fields, yielding flight times inconsistent with their real kinetic energy. To counteract this issue, the chamber was built out of μ-metal and described in [15]. As schematically shown in Figure 1, two ETF20 Kaesdorf electron time-of-flight (eTOF) spectrometers measured the strength of the streak induced on the photoelectrons by the vector potential of the THz field. This tandem measurement is used to eliminate the photon energy jitter common at FELs from the observed spectra. The pressure near the sensor element of the eTOFs, the multi-channel plates (MCPs) should not be on the order of 10^{-6} mbar to prevent sparking and damage to the MCPs. Small pumps are attached to the eTOFs to keep the drift tube under low pressure despite a higher gas load in the chamber. Despite this precaution, the pressure in the main chamber is limited by the tolerance of the MCPs, and should always be checked before the device is started.

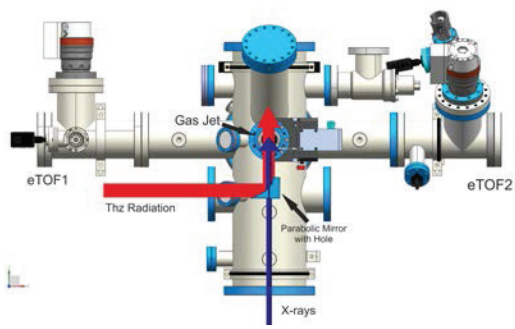

Figure 1: Schematic drawing of the PALM prototype chamber.

The two e-TOF spectrometers, positioned opposite each other, measure exact opposite streaking effects, but measure the same electron kinetic energy shift due to photon energy jitter. The resolution of the eTOFs over the dynamic range of the measurement is controlled by adjusting their drift tube and electrostatic lens settings. By subtracting the average of the two mean kinetic energies from each individual measurement, the photon energy jitter contribution is eliminated, leaving only the clean measurement of the FEL relative pulse arrival time.

The Xe gas is injected into the interaction region by a LaserLab Amsterdam piezo cantilever valve [21] synchronously with the FEL repetition rate. The valve has a 40° conical nozzle with a diameter of 150 μm with a backing pressure of about 3.5 bar above atmospheric pressure. The valve was placed 10 to 12 mm away from the center of the interaction region to deliver the largest amount of gas in the smallest volume possible while not interfering with the flight path of either the THz beam or the FEL pulse. The estimated diameter of the gas target in the interaction region was between 1.2 and 1.5 mm. The average pressure in the chamber while the valve was working was 1.1×10^{-5} mbar, with a background pressure of about 3×10^{-7} mbar.

The THz radiation has thus far been generated in a $LiNbO_3$ crystal via the tilted pulse-front pumping method [22] optimized for a high-energy pump [23] by 800 nm laser 5-10 mJ system outside of the chamber and then introduced into vacuum through a z-cut quartz window. The laser intensity should be monitored on a shot-to-shot basis to compensate for the change in the THz field's power in the data analysis. A three inch parabolic mirror focuses the THz radiation 170 mm downstream, 20 mm behind the interaction region to avoid Gouy phase shift [24] effects across the diameter of the gas target. The unfocused x-ray FEL pulses are transmitted though the 3-5 mm hole in the middle of the parabolic mirror and co-propagate with the THz field. High humidity or temperature variations can have an effect on the laser power or the strength of the THz field, so utmost care should be taken to stabilize both in the room the PALM is placed in. A larger streaking slope gives better results and time resolution.

The setup of the device requires a calibration of the eTOFs to find an accurate electron flight-time to kinetic energy scale. This is done by either scanning the photon energy of the FEL beam over several hundred electron volts, a hard and time-consuming process for the operators, or by tweaking the retardation voltage settings on the eTOFs to simulate an effective lower photon energy by directly reducing the kinetic energy of the electrons in the flight tube. The latter method works best for high kinetic energy electrons (>1000 eV) so that the flight time from the interaction region to the entrance of the eTOF is as short as possible. Lower energies have larger variations in flight times over this field-free region, and would not be well-simulated by altering only the flight time in the flight tube.

The calibration scan should also record the measured spectral width as a function of retarded energy. The eTOF lensing and retardation systems are usually optimized around one energy—large variations from this sweet spot cause de-focusing effects from the electrostatic lenses, yielding larger measured electron kinetic energy spectral widths than what the FEL delivered. This effect can be corrected for by measuring the response of the spectral width as a function of electron kinetic energy for a single photon energy, and then accounted for in analysis later. One such scan is shown in Figure 2.

ISBN 978-3-95450-133-5

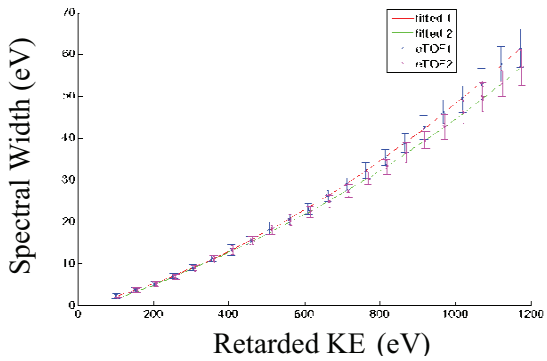

Figure 2: ETOF spectral width scan for 7 keV with a monochromator done at SACLA.

Further tests need to be done to check the accuracy of measurement of the mean kinetic energy of a peak, performed by having to eTOFs measure the same beam at the same time without the THz streak and comparing the variations of the kinetic energies they measure. This measurement is typically accurate to about 0.3-1% of the retarded kinetic energy of the electrons.

ANALYSIS CONSIDERATIONS

There are several effects that have to be accounted for when evaluating the data from a THz streak camera measurement. Some of the most important ones are listed below, along with some suggestions mitigate them.

Spectral width drift and jitter is the tendency of the FEL beam to change the width of its spectrum with time or on a shot-to-shot basis. If a calibration measurement was done with one spectral width, and the beam changes this width, the final evaluation for pulse length can be erroneous. The addition of another e-TOF that would measure the non-streaked beam would rectify this problem, seeing any drifts or jitters in the on a shot-by-shot basis.

Space charge is generated in the interaction region as the thousands or millions of atoms are photoionized by the FEL beam. The effect is most easily observed for electrons of low kinetic energies, where even a small space charge can retard the flight of an electron to a measurable degree. High energy electrons, however, are much less sensitive to the space-charge effect, and the few-eV space charge contribution to the streaking strength of a multi-keV electron is negligible.

A large number of electrons flying together through the drift tube of the eTOF have mutual Coulomb repulsions which could distort the original imprint the FEL pulse created at the time of photoionization. This can cause the perceived spectral width to be larger than the real one. However, simulations done with SimION have shown that the contribution from such repulsions for 1000-2000 high-KE electrons flying simultaneously through the drift tube, a number that is typical for a single peak observed by the eTOFs, is small, on the level of a percent or less of the spectral width. The effect is noticeable for low kinetic energy electrons (few eV-10s of eV) since they have more time to separate themselves in the drift tube.

CONCLUSIONS

The PSI-developed PALM device will measure the arrival time and pulse length of hard x-rays at SwissFEL. Because it is a gas-based measurement method, it is also less intrusive than most other methods and allows for the use of the FEL pulse for experiments further downstream with a minimal loss of intensity or wavefront distortion.

REFERENCES

[1] W. Ackermann et. al., "Operation of a free-electron laser from the extreme ultraviolet to the water window," *Nature Photonics,* vol. 1, p. 336, 2007.

[2] P. Emma et. al., "First lasing and operation of an angstrom-wavelength free-electron laser," *Nature Photon,* vol. 4, p. 641, 2010.

[3] D. Pile et. al., "X-rays first light from SACLA," *Nature Photon,* vol. 5, p. 436, 2011.

[4] E. Allaria et. al., "The FERMI@Elettra free-electron-laser source for coherent x-ray physics: photon properties, beam transport system and applications," *New J. Phys,* vol. 12, p. 075002, 2010.

[5] P. Oberta et. al., "The SwissFEL facility and its preliminary optics beamline layout," *Proceedings of SPIE,* vol. 8079, p. 807805, 2011.

[6] M. Bionta et. al., "Spectral encoding of x-ray/optical relative delay," *Optics Express,* vol. 19, p. 21855, 2011.

[7] M. Beye et. al., "X-ray pulse preserving single-shot optical cross-correlation method forimproved experimental temporal resolution," *Appl. Phys. Lett.,* vol. 100, p. 121108, 2012.

[8] O. Krupin et. al., "Temporal cross-correlation of x-ray free electron and optical lasers usingsoft x-ray pulse induced transient reflectivity," *Optics Express,* vol. 20, p. 11396, 2012.

[9] M. Harmand et. al., "Achieving few-femto second time-sorting at hard X-ray free-electron lasers," *Nature Photon.,* vol. 7, pp. 215-218, 2013.

[10] I. Grguras et. al., "Utrafast X-ray pulse characerization at free electron lasers," *Nature Photon,* vol. 6, p. 852, 2012.

[11] U. Frühling et. al., "Single-Shot Terahertz-Field-Driven X-ray Streak Camera," *Nature Photon,* vol. 3, p. 353, 2009.

[12] F. Tavella et. al., "Few-femtosecond timing at fourth-generation X-ray light sources," *Nature Photon,* vol. 5, p. 162, 2011.

[13] S. Duesterer et. al., "Femtosecond x-ray pulse length characterization at the Linac Coherent Light Source free-electron laser," *New J. Phys,* vol. 13, p. 093024, 2011.

[14] R. Riedel et. al., "Single-shot pulse duration monitor for exterme ultraviolet and X-ray free electron lasers," *Nature Comm.,* vol. 4, p. 1731, 2013.

ISBN 978-3-95450-133-5

[15] P. Juranic et. al., "A scheme for a shot-to-shot, femtosecond-resolved pulse length and arrival time measurement of free electron laser x-ray pulses that overcomes the time jitter problem between the FEL and the laser," *JINST,* vol. 9, p. P03006, 2014.

[16] M. Hentschel et. al., "Attosecond Metrology," *Nature,* vol. 414, p. 509, 2001.

[17] M. Drescher et. al., "X-ray pulses approaching the attosecond frontier," *Science,* vol. 291, p. 1923, 2001.

[18] M. Uiberecker et. al., "Attosecond Metrology with Controlled Light Waveforms," *Laser Physics,* vol. 15, p. 195, 2005.

[19] B. L. Henke, E. M. Gullikson and J. C. Davis, "X-ray interactions: photoabsorbtion, scattering, transmission, and reflection at E=50-30,000 eV, Z=1-92," *At. Data Nucl. Data Tables,* vol. 54, pp. 181-342, 1993.

[20] G. N. Makarov and A. N. Petin, "Investigation of Atomic and Molecular Clustering in a Pulsed-Gas Dynamic Jet with a Pyroelectric Detector," *Journal of Experimental and Theoretical Physics,* vol. 107, pp. 725-733, 2008.

[21] D. Irimia et. al., "A short pulse (7msFWHM) and high repetition rate (dc-5kHz) cantilever piezovalve for pulsed atomic and molecular beams," *Rev. Sci. Inst.,* vol. 80, p. 113303, 2009.

[22] J. Hebling et. al., "Velocity matching by pulse front tilting for large area THz-pulse generation," *Opt. Express,* vol. 10, pp. 1161-1166, 2002.

[23] A. G. Stepanov et. al., "Mobile source of high-energy single-cycle terahertz pulses," *Appl. Phys. B,* vol. 101, pp. 11-14, 2010.

[24] A. B. Ruffin et. al., "Direct Observation of the Gouy Phase Shift with Single-Cycle Terahertz Pulses," *Phys. Rev. Lett.,* vol. 17, p. 3410, 1999.

ISBN 978-3-95450-133-5